Study of Immune Colloidal Silver Rapid Detection of Melamine

Kuo-Hui Wu^{1*}, Wen-Chien Huang² and Yin-Chiung Chang³

¹Department of Chemical and Materials Engineering, Chung Cheng Institute of Technology, National Defense University, Taoyuan 335, Taiwan

ABSTRACT

Melamine contamination of food or food-related products is a major global food safety issue, posing a serious threat to human health. An immunochromatography test strip (ICTS) for the rapid detection of melamine using colloidal silver (Ag-TSC) as the signal material was developed. The method of preparation of the antibody–colloidal silver conjugate was based on the ionic interactions binding antibodies with colloidal silver. Morphological study by SEM and TEM showed that the average size of the uniform spherical immune colloidal silver particles (Ag-TSC-mAb) was 20~30 nm. The spectroscopic properties of Ag-TSC showed the typical surface plasmon resonance band at 387 nm in the UV-visible spectrum. FTIR analyses indicated that citrate anions and anti-MEL monoclonal antibodies were adsorbed on the Ag-TSC through carboxylate groups. The mAb conjugated with the colloidal silver, and was applied to the conjugate pad of the ICTS. The visual detection limit for the ICTS was 0.5 ppm. No cross-reactions with homologues cyanuric acid, ammeline or ammelide were found, and this test required only 15 min to obtain a result. The ICTS can be prepared simply, and provides an alternative tool for sensitive, rapid, convenient and semi-quantitative detection of the analyte on-site.

Keywords: Immunochromatography Test Strip, Colloidal Silver, Trisodium Citrate, Melamine.

免疫膠體銀快速檢測三聚氰胺之研究

吳國輝 ^{1*} 黃文鍵 ² 張尹瓊 ³

¹國防大學理工學院化學及材料工程學系 ²國防大學理工學院國防科學研究所 ³陸軍專科學校化學工程科

摘 要

三聚氰胺對食品或食品相關產品的污染是重大的全球食安議題,對人類健康構成嚴重威脅。以膠體銀(Ag-TSC)為信號材料應用於快速檢測三聚氰胺的免疫層析試紙(ICTS)開發。基於離子相互作用方法將抗體與膠體銀相結合,完成抗體-膠體銀偶聯體製備。藉由 SEM 和TEM 研究發現,免疫膠體銀(Ag-TSC-mAb)呈現均勻球形狀,平均粒徑為 20~30 nm。紫外-可見光譜在 387 nm 處顯示膠體銀典型的表面電漿子共振吸收。FTIR 分析則發現檸檬酸根陰離

²School of Defense Science, Chung Cheng Institute of Technology, National Defense University, Taoyuan 335, Taiwan

³Department of Chemical Engineering, Army Academy, 32092, Taoyuan, Taiwan

文稿收件日期 108.1.22;文稿修正後接受日期 108.11.22;*通訊作者 Manuscript received January 22, 2018; revised November 22, 2019; * Corresponding author

子和抗三聚氰胺單克隆抗體通過羧酸根基團吸附在膠體銀上。免疫膠體銀被應用於 ICTS 的結合墊上,經檢測發現,該試紙的視覺檢測極限為 0.5 ppm。沒有發現與同系物三聚氰酸,三聚氰酸一醯胺或三聚氰酸二醯胺的交叉反應,並且該檢測時間僅需 15 分鐘即可獲得結果。ICTS可以被簡單製備並作為現場檢測分析物的替代工具,具有靈敏、快速、方便和半定量等優點。

關鍵詞:免疫層析試紙,膠體銀,檸檬酸三鈉,三聚氰胺

I. INTRODUCTION

An immunochromatography test (ICTS), often called a strip assay or a lateralassav, based is immunochromatographic procedure that utilizes antigen and antibody properties and provides rapid detection of an analyte [1]. An ICTS requires the least sample pretreatment, without the need for expensive equipment, and the results can be obtained within 15 min. Colloidal gold-based immunochromatographic assays are the most widely-used methods for the detection of specific compounds [2,3]. The development of nanotechnology has resulted in new methods and approaches for the design of rapid, accurate and sensitive diagnostic techniques in recent years. Colloidal silver (Ag-TSC) is of great interest in nanotechnology, and has been employed in a wide range of ICTS applications due to its unique optical properties and surface chemistry [4,5].

Melamine (1,3,5-triazine-2,4,6-triamine, C₃H₆N₆, MEL) is a typical polar organic triazine compound. It is an industrial chemical employed in the production of plastics, fire retardant materials and amino resins. Owing to its high melamine nitrogen content, has intentionally added to milk, milk powder and other cereal-based ingredients used for pet food and feed in order to artificially increase the apparent protein content. Although low levels of melamine do not cause any danger to humans. excessive intake of melamine above the safe limit can induce renal failure [6]. It has been reported that poisonous pet foods, feeds and infant formula resulting from deliberate MEL contamination have severely impacted the health of thousands of pets and babies in 2004, 2007 and 2008, and this has become a worldwide concern [7].

MEL contamination of food or food-related products is mainly assessed by means of

analysis instrumental such gas chromatography mass spectrometry (GC/MS), chromatography/tandem spectrometry (LC/MS/MS), high-performance liquid chromatography (HPLC), enzyme-linked immunosorbent assay (ELISA) electrochemical. Despite the high sensitivity and specificity that can be achieved by the GC/MS, LC/MS/MS, HPLC, ELISA and electrochemical methods, these analytical methods demand skilled laboratory technicians and take much time to achieve a confirmed identification [8,9].

In this work, we report the preparation of antibody-colloidal silver conjugates. Using these conjugates, we not only developed a lateral-flow immunoassay method, but also established an ICTS to detect melamine. The ICTS can be prepared simply, and provides an alternative tool for sensitive, rapid, convenient and semi-quantitative detection of the analyte on-site.

II. EXPERIMENTAL SECTION

2.1 Materials and reagents

Silver nitrate (AgNO₃) and trisodium citrate dihydrate (TSC) were purchased from J.T. Baker Chemical Sodium Company. borohydride ammelide (NaBH4), cyanuric acid, ammeline were purchased from Sigma-Aldrich. Trehalose was purchased from Alfa Aesar. Bovine serum albumin (BSA) was purchased from Jackson ImmunoResearch Inc. Polyoxyethylene sorbitan monolaurate (Tween-20) was purchased from Bio Basic Canada INC. Melamine (MEL), BSA-melamine conjugate, anti-MEL monoclonal antibody (mAb), goat immunoglobulin anti-rabbit G nitrocellulose membrane (NC membrane), sample pads and absorbent pads were purchased from Advance Bio-Pharmaceutical Inc. (Taiwan). All chemicals were of analytical grade and were

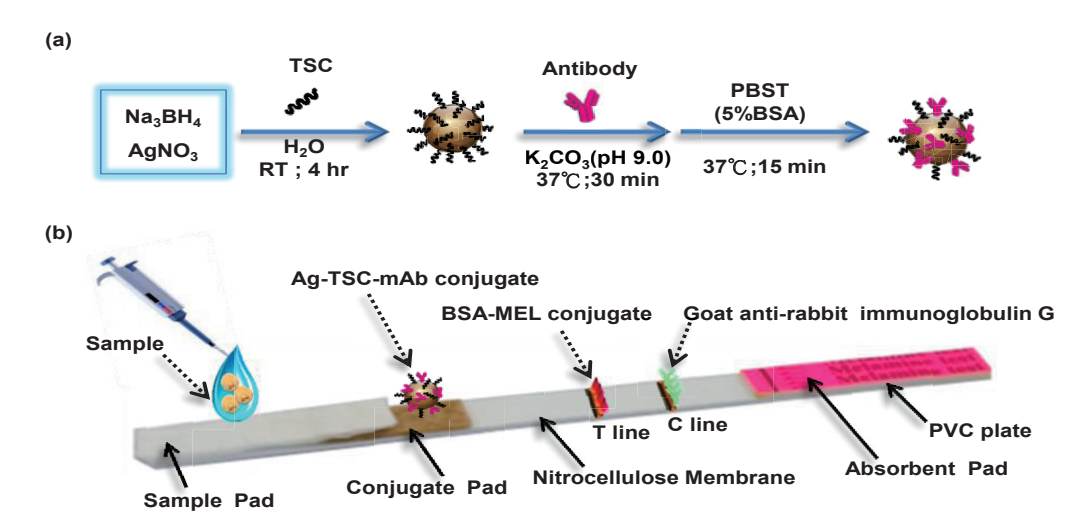


Fig.1. (a) Schematic route for the synthesis of Ag-mAb and (b) the preparation and assemblage of the ICTS.

used without further purification. The following buffers were prepared by us: (1) phosphate-buffered saline (PBS) was used, at pH 7.4, containing 8.00 g NaCl, 0.20 g KCl, 1.42 g Na₂HPO₄ and 0.27 g KH₂PO₄. (2) PBST solution was used, at pH 7.4, containing 99.90% PBS solution and 0.1% Tween-20. (3) A conjugate pad solution was used, at pH 7.4, containing 99.00% PBS solution, 0.1% BSA, 10.00% trehalose and 0.05% Tween-20.

2.2 Preparation of Ag-TSC probes and conjugation of antibody

Ag-TSC was synthesized by a simple chemical reduction method using NaBH4 as the reducing agent. Briefly, 10.0 mL of 0.001 M AgNO₃ were added drop-wise (at about 1 drop per second) to 30.0 mL of 0.002 M NaBH₄ solution. Next, 1 mL of 0.02 M TSC solution was added to stabilize the silver nanoparticles. The reaction was allowed to continue for 4 hours, and the solution turned from bright yellow to brown.

The pH of Ag-TSC was adjusted to 9.0 with 0.1 M K₂CO₃ (potassium carbonate). Then, 60 μL of 1.0 mg mL⁻¹ mAb were added in drops to 10.0 mL Ag-TSC solution. The solution was gently mixed at 37°C for 1 hour, blocked by 2.5 mL of 5.0 wt.% BSA solution for 15 min, and then centrifuged (at 6,000 rpm for 20 min) to remove the supernatant of unconjugated antibodies. The pellet obtained was washed with PBST once again. Finally, Ag-TSC-mAb was

redispersed in 50 μ L PBS (pH 7.4) and stored at 4°C (Figure 1 (a)).

2.3 Characterization of Ag-TSC and the Ag-TSC-mAb conjugate

The formation of an Ag-TSC-mAb conjugate was confirmed by Fourier transform Infrared (FTIR, Perkin Elmer Spectrum 100) and UV-Vis Shimadzu, (UV3101PC, Kyoto, Japan) spectrophotometry. The morphologies Ag-TSC and the Ag-TSC-mAb conjugate were characterized by scanning electron microscopy (SEM, JSM-6330F) and transmission electron microscopy (TEM, Hitachi H-7100), in which SEM and TEM images were used to physically measure the size of Ag-TSC and the Ag-TSCmAb conjugate. Optical images of the test strips were acquired using a camera and then processed using Image J software for analysis of the optical density of the test line. Optical images were acquired using a Smart phone (ASUS), and then processed using ImageJ 1.51j8 software to analyze the optical density from the test line (T) and control lines (C).

2.4 Preparation of the immunochromatography test strip

The preparation and assemblage of the immunoassay test device is shown in Figure 1 (b). Briefly, The NC membrane on which capture reagents, e.g., BSA-MEL and goat antirabbit IgG, were immobilized was an important

element of the test strip. BSA-MEL conjugate (0.4 mg mL⁻¹) and goat anti-rabbit IgG (1.0 mg mL⁻¹) were separately applied to the NC membrane and used as the test line and the control line, respectively. The Ag-TSC-mAb conjugate pad was prepared by immobilizing Ag-TSC-mAb conjugate onto the conjugate pad. First, the conjugate pad was treated with conjugate pad solution for 30 min and dried for 2 hours at 37°C. Then, 2 uL of Ag-TSC-mAb conjugate solution were spotted on the conjugate pad. The resultant conjugate pad was incubated at 37°C for 1 hour until fully dried. A PVC plate served as the bottom (backing) of the test strip. The NC membrane was pasted onto the center of the PVC plate, and the Ag-TSC-mAb conjugate pad was pasted onto the plate with an overlap of 5 mm with the NC membrane. An absorbent pad and sample pad were pasted on the two sides of the ICTS. Strips were then sealed in a plastic bag in the presence of desiccant gel and stored at room temperature.

2.5 Sensitivity and specificity of the immunochromatography test strip

For the sensitivity assay, $100~\mu L$ samples containing different amounts of MEL (0, 0.1, 0.3, 0.5, 0.7) and 0.9~ppm) were applied onto the ICTS. For the specificity test, samples containing 5 ppm of various substances (melamine, cyanuric acid, ammeline and ammelide) were all assayed using the ICTS.

Ⅲ. RESULTS AND DISCUSSION

3.1 Characterization of Ag-TSC and the Ag-TSC-mAb conjugate

The optical properties of Ag-TSC are highly-dependent on the nanoparticle diameter and refractive index near the nanoparticle surface. The particles were synthesized by chemical reduction of AgNO₃ using NaBH₄ [10]. The borohydride anions were adsorbed onto the silver nanoparticles, and the addition of TSC prevented aggregation of particles. A brown color was imparted by the Ag-TSC solution, which had a surface plasmon resonance (SPR) at 387 nm according to spectrophotometry. The Ag-TSC particles were estimated to be 15~30 nm in diameter (Figure 2).



Fig.2. The colloidal silver as it appears to the naked eye.

UV-Vis absorption spectroscopy was a simple and efficient method by which to verify the formation of the Ag-TSC-mAb conjugates. It has been noted that the shape and location of the plasmonic band in the UV-Vis spectrum could differ depending on the size and polydispersity of the nanoparticles formed [11]. The citratecapped silver nanoparticles presented surface plasmon resonance bands (SPRs) at 387 and 428 nm (Figure 3 (a)). The first peak, situated at 387 nm, was attributed to the SPR band of Ag-TSC, while the second peak, at 428 nm, was attributed to the larger silver nanoparticles. The citratesilver nanostructures terminated Ag-TSC-mAb conjugates by a ligand exchange reaction of anti-MEL mAb. The SPRs of the Ag-TSC-mAb conjugates shifted to higher wavelengths of 393 and 449 nm (Figure 3 (b)), with a decrease in the absorbance value. This indicated that, after reacting with mAb, agglomeration of silver nanoparticles occurred in part. This was supported by TEM and SEM measurements.

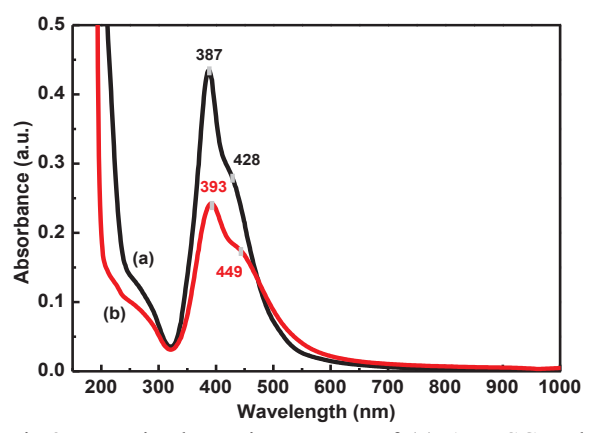


Fig.3. UV-Vis absorption spectra of (a) Ag-TSC and (b) Ag-TSC-mAb.

The high stability of the antibody-stabilized silver nanoparticles was further confirmed by TEM and SEM characterization. As shown in

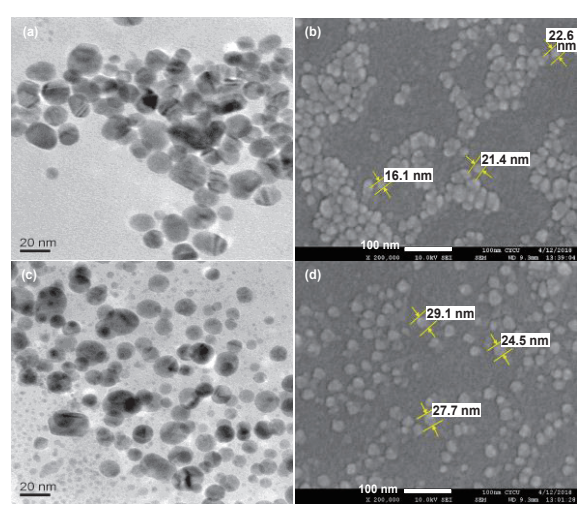


Fig.4. (a) TEM image and (b) SEM micrographs of the Ag-TSC, (c) TEM image and (d) SEM micrographs of the Ag-TSC-mAb.

Figure 4, it was clearly observed that the dispersity of the Ag-TSC-mAb conjugate was fine, with significantly less aggregation than the Ag-TSC conjugate. Most of the Ag-TSC and Ag-TSC-mAb conjugates displayed well-distributed spherical nanocrystals, with diameters below 25 and 30 nm, respectively. It is worthy of note that the average hydrodynamic diameter of Ag-TSC-mAb increased from 15 nm to 30 nm.

Figure 5 depicts the FTIR spectra and second derivative IR spectra of the Ag-TSCmAb conjugate. The TSC spectra showed a broad peak at around 3376 cm⁻¹, which indicated OH stretching. In the spectra, two prominent peaks at 1566 and 1392 cm⁻¹ were observed, which arose from the asymmetrical and symmetrical stretching of COOrespectively (Figure 5 (a)). The absorption bands of the Ag-TSC nanoparticles at 1650, 1558 and 1392 cm⁻¹ were attributed to the antisymmetric and symmetric stretching vibrations of COO on the surface of the silver nanoparticles (Figure 5) carboxylate ion usually (a)) [12]. The coordinates to metal ions in three main ways: unidentate, bidentate and bridging. In general, the Δv , $v_{as}(COO^{-}) - v_{s}(COO^{-})$, is indicative of the binding characteristic of a carboxylate group with a metal ion. The values of $\Delta v = v_{as}(COO^{-})$ – $v_s(COO^-)$ with a high probability monodentate complexes are expected to be much larger than 200 cm⁻¹, or much greater than those of ionic complexes. In most cases, complexes with $\Delta v < 200$ possess chelating and/or bridging carboxylate groups. From the FTIR

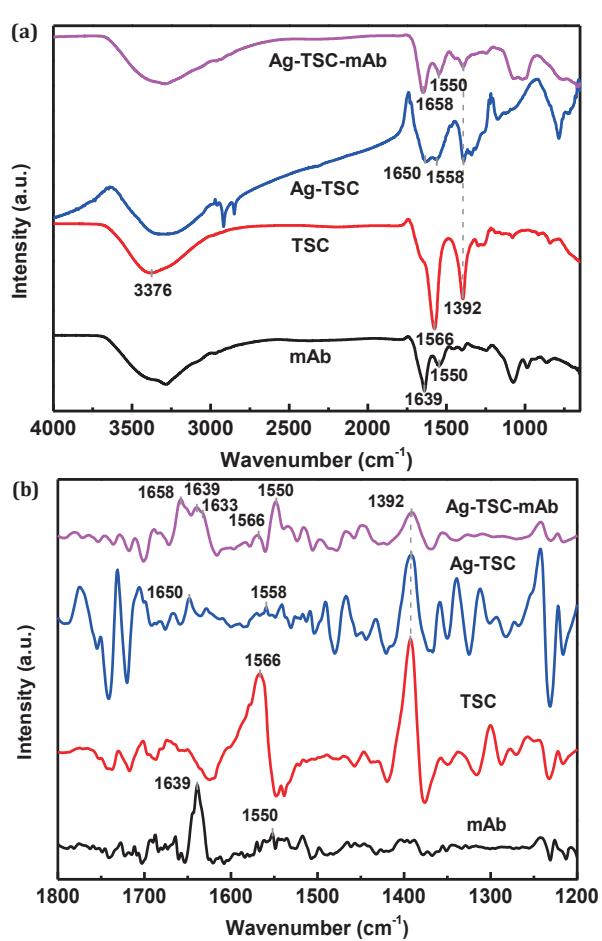


Fig.5. (a) FTIR spectra and (b) second derivative IR spectra of Ag-TSC-mAb conjugate.

spectra of carboxylic groups, it is possible to determine monodentate or chelating and/or bridging bonds in metal complexes, and also the nature of the Ag-ligand bond [13]. In our experiment, the Δv values of the Ag-TSC nanoparticles were 258 and 166 cm⁻¹, respectively, with two bonding structures of the bridged and monodentate type. For the mAb samples, the FTIR bands at 1639 and 1550 cm⁻¹ corresponded with the amide I band and, respectively, the amide II band (Figure 5 (a)) [14]. In the case of the Ag-TSC-mAb conjugate, the absorption bands at 1658 and 1566 cm were attributed to the antisymmetric and, respectively, symmetric stretching vibrations of COO of the citrate molecule present on the surface of the silver nanoparticles. Furthermore, the absorption band at 1633 cm⁻¹ was attributed to the antisymmetric symmetric stretching vibrations of COO of mAb present on the surface of the silver nanoparticles. The mAb sample absorption bands were also present in the

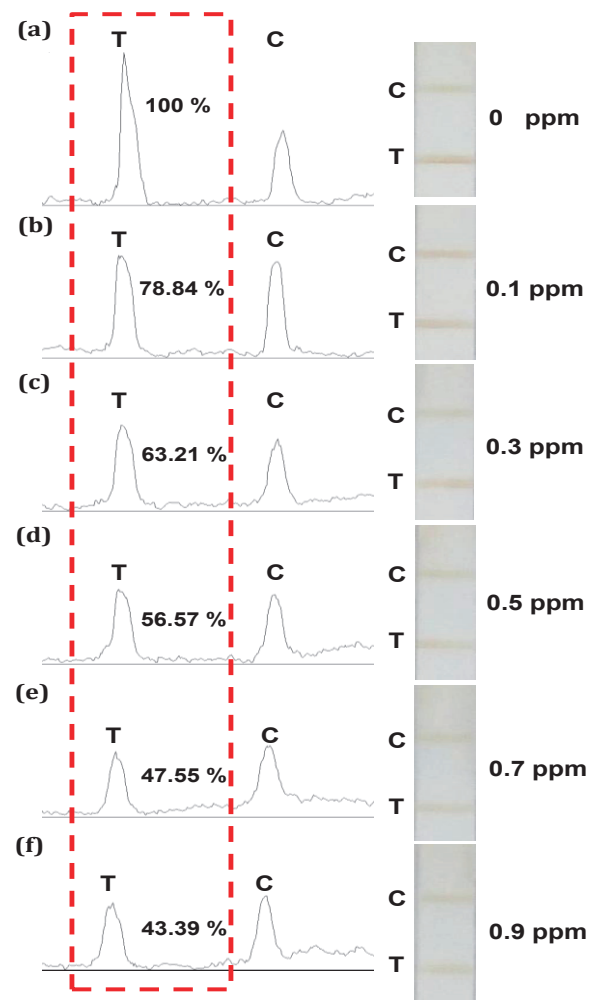


Fig.6. Concentration range of MEL standard assayed by the immuneochromatographic strip tests.

final bio-nanocomposite at 1639 and 1550 cm⁻¹, rendering the FTIR spectra of mAb and Ag-TSC-mAb almost identical (Figure 5 (b)). Thus, in the case of the Ag-TSC-mAb conjugate, corroboration of the appearance of mAb characteristic FTIR bands confirmed the successful functionalization of silver nanoparticles with mAb.

3.2 Sensitivity of the immunochromatography test strip

Figure 6 presents typical photographic images (right) and the corresponding optical response recorded with Image J software in the presence of different concentrations of MEL (0 to 0.9 ppm). Based on optimal assay conditions, MEL standard solutions were detected by the ICTS in triplicate. The intensity of the brown color on the test lines was reduced as the concentration of

MEL increased. Herein, the visual detection limit was defined as the minimum target analyte concentration required for the test line to show no obvious staining effect [15]. The intensity of the brown color on the test line at 0.5 ppm of MEL was significantly weaker than that at zero concentration. Thus, 0.5 ppm of MEL was considered to be the visual detection limit for the ICTS, which is below the detection limit that is legislated by the European Union (EU) and the Food and Drug Administration (FDA) [9]. Because human visual limits was prone to make deviation, digital images taken with digital cameras are used for grayscale analysis to quantify and improve detection sensitivity. The immune colloidal silver-based ICTS images were analyzed by integrating the cross-section of the test line and control line using ImageJ software. By defining the detection limit as the minimum concentration of analyte required to induce a 10% relative optical signal decrease [16], the limit was determined to be 0.1 ppm for the ICTS.

3.3 Specificity of the immunochromatography test strip

The specificity of cyanuric acid, ammeline and ammelide on the ICTS was assayed in triplicate. The results showed that only MEL produced a positive result. Negative results were obtained for cyanuric acid, ammeline and ammelide (Figure 7), indicating clear specificity of the ICTS.

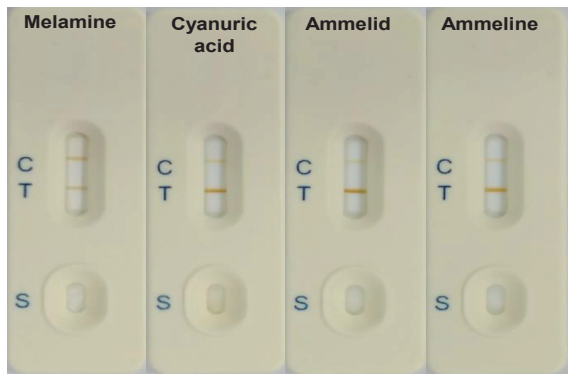


Fig.7. The cross-reaction of the MEL test strip with Melamine, Cyanuric acid, Ammelid and Ammeline.

IV. CONCLUSION

The present study demonstrated a new

approach towards the development of immunoassay-based dipsticks, which makes use of silver nanoparticles as the detection reagent. The ICTS can be prepared by a simple and convenient method, and is able to detect MEL contamination rapidly, sensitively, and without cross-reaction with homologues. Results were obtained within 15 min without expensive equipment. 0.5 ppm of MEL was considered to be the visual detection limit for the ICTS, which was below the detection limit that is legislated by the European Union (EU) and the Food and Drug Administration (FDA). The assay format can be easily extended to other toxins by controlling the target antibody.

ACKNOWLEDGEMENTS

The authors thank the Ministry Science and Technology for supporting this work (MOST 107-2623-E-606-006-D).

REFERENCES

- [1] Zhang, L., Huang, Y., Wang, J., Rong, Y., Lai, W., Zhang, J., and Chen, T., "Hierarchical Flowerlike Gold Nanoparticles Labeled Immunochromatography Test Strip for Highly Sensitive Detection of Escherichia coli O157:H7," Langmuir, Vol. 31, No. 19, pp. 5537-5544, 2015.
- [2] Gong, Y., Zhang, M., Wang, M., Chen, Z., and Xi, X., "Development of Immuno-Based Methods for Detection of Melamine," Arabian Journal for Science and Engineering, Vol. 39, No. 7, pp. 5315-5324, 2014.
- [3] Zhong, Y., Chen, Y., Yao, Li., Zhao, D., Zheng, L., Liu, G., Ye, Y., and Chen, Wei., "Gold nanoparticles based lateral flow immunoassay with largely amplified sensitivity for rapid melamine screening," Microchimica Acta, Vol. 183, No. 6, pp. 1989-1994, 2016.
- [4] Liang J., Liu H., Lan C., Fu Q., Huang C., Luo Z., Jiang T., and Tang Y., "Silver nanoparticle enhanced Raman scattering-based lateral flow immunoassays for ultrasensitive detection of the heavy metal chromium," Nanotechnology, Vol. 25, No.

- 49, pp. 495501, 2014.
- [5] Panferov V. G., Safenkova I. V., Byzova N. A., Varitsev Y. A., Zherdev A. V., and Dzantiev B. B., "Silver-enhanced lateral flow immunoassay for highly-sensitive detection of potato leafroll virus," Food and Agricultural Immunology, Vol. 29, pp.1-13, 2017.
- [6] Li, X., Luo, P., Tang, S., Beier, R. C., Wu, X., Yang, L., Li, Y. and Xiao, X., "Development of an Immunochromatographic Strip Test for Rapid Detection of Melamine in Raw Milk, Milk Products and Animal Feed," Journal of Agricultural and Food Chemistry, Vol. 59, pp. 6064-6070, 2011.
- [7] Wang, Z., Zhi, D., Zhao, Y., Zhang, H. A., Wang, X., Ru, Y., and Li, H. O., "Determination and Confirmation of Melamine Residues in Catfish, Trout, Tilapia, Salmon, and Shrimp by Liquid Chromatography with Tandem Mass Spectrometry," International Journal of Nanomedicine, Vol. 9, pp. 1699-1707, 2014.
- [8] Andersen, W. C., Turnipseed, S. B., Karbiwnyk, C. M., Clark, S. B., Madson, M. R., Giessker, C. M., Miller, R. A., Rummel, N. G., and Reimschuessel, R., "Silver nanoparticle enhanced Raman scatteringbased lateral flow immunoassays for ultrasensitive detection of the heavy metal chromium," Journal of Agricultural and Food Chemistry, Vol. 56, No. 12, pp. 4340-4347, 2008.
- [9] Lu, Y., Xia, Y., Liu, G., Pan, M., Li, M., Lee, N. A., and Wang, S., "A review of methods for detecting melamine in food samples," Critical Reviews in Analytical Chemistry, Vol. 47, No. 1, pp. 51-66, 2017.
- [10] Mavani, K., and Shah, M., "Synthesis of Silver Nanoparticles by using Sodium Borohydride as a Reducing Agent," International Journal of Engineering Research & Technology, Vol. 2, No. 3, pp. 1-5, 2013.
- [11] Mineva, Bc. A., "Characterization of size of polydisperse nanoparticles of various shape:

 Comparative study of AFM and DLS methods," Unpublished undergraduate dissertation, Czech Technical University, Prague, 2017.
- [12] Park, J. W., and Shumaker-Parry, J. S.,

- "Structural Study of Citrate Layers on Gold Nanoparticles: Role of Intermolecular Interactions in Stabilizing Nanoparticles," Journal of the American Chemical Society, Vol. 136, No. 5, pp. 1907-1921, 2014.
- [13] Azócar, M.I., Gómez, G., Levín, P., Paez, M., Muñoz, H., and Dinamarca, N., "REVIEW: Antibacterial behavior of silver(I) complexes," Journal of Coordination Chemistry, Vol. 67, pp. 3840-3853, 2014.
- [14] Matea, C.T., Mocan, T., Zaharie, F., Iancu, C,. and Mocan, L., "A novel immunoglobulin G monolayer silver bionanocomposite," Chemistry Central Journal, Vol. 9, pp. 55-62, 2015.
- [15] Liu, C., Ma, W., Gao, Z., Huang, J., Hou, Y., Xu, C., Yang, W., and Gao, M., "Upconversion luminescence nanoparticlesbased lateral flow immunochromatographic assay for cephalexin detection," Journal of Materials Chemistry C, Vol. 2, pp. 9637-9642, 2014.
- [16] Liu, C., Jia, Q., Yang, C., Qiao, R., Jing, L., Wang, L., Xu, C., and Gao, M., "Lateral Flow Immunochromatographic Assay for Sensitive Pesticide Detection by Using Fe₃O₄ Nanoparticle Aggregates as Color Reagents," Analytical Chemistry, Vol. 83, No. 17, pp. 6778-6784, 2011.